2024 IEEE International Symposium on Biomedical Imaging (ISBI) | 979-8-3503-1333-8/24/$31.00 ©2024 IEEE | DOI: 10.1109/ISBI56570.2024.10635720

PRECISION DIAGNOSIS OF AUTISM THROUGH RESTING FMRI AND MACHINE LEARNING

Mohamed Khudri[1], *Mostafa Abdelrahim*[1], *Mohamed T. Ali*[2], *Yaser A. Elnakib*[2], *Ahmed Shalaby*[3], Ali Mahmoud[1], Sohail Contractor[4], Gregory N. Barnes[5], and Ayman El-Baz[1]

[1]Bioengineering Department, University of Louisville, KY, USA
[2] Clinical Informatics Center UTSW Medical Center, Dallas, TX, USA
[3] Lyda Hill Department of Bioinformatics,UTSW Medical Center, Dallas, TX, USA
[4] Department of Radiology, University of Louisville, Louisville, KY, USA
[5] Department of Neurology, University of Louisville, Louisville, KY, USA

ABSTRACT

In this paper, we present a pioneering diagnostic system that utilizes resting state Functional Magnetic Resonance Imaging (fMRI) and Machine Learning (ML) to effectively evaluate individuals with autism spectrum disorder (ASD). Our system's primary objective is to assess the severity of autism by accurately identifying specific brain regions that demonstrate robust correlations with the behavioral patterns observed in autistic subjects. The proposed system involves several essential steps: i) It begins by preprocessing fMRI data to correct head motion, reduce susceptibility distortion in the reconstructed BOLD signal, and align the subject's fMRI with their structural MRI, thereby improving fMRI resolution. ii) Following this, the brain cortex is extracted from the aligned fMRI using its sMRI. iii) The brain is then divided into 76 areas per hemisphere using MNI152 standard space. To identify brain areas associated with ASD, fMRI radiomics employs estimating the correlation matrix, outlining the mutual synchronization between each pair of brain regions. v) Areas significantly correlated with ASD, at a 95% confidence interval, are pinpointed using the Recursive Feature Elimination (RFE) algorithm. vi) Lastly, the final step involves using the Linear support vector machine (LSVM) to diagnose each subject as normal or autistic, determining their respective severity levels, and identifying abnormal brain regions crucial in detecting abnormal neurocircuits that play a pivotal role in managing autism. The proposed approach was tested on 344 with ASD and 374 typically developing individuals from the Autism Brain Imaging Data Exchange II (ABIDE II). Through 5-fold cross-validation, the proposed system attained 97% accuracy, 90% sensitivity and 0.99% specificity.

***Index Terms*—** Autism, resting state fMRI, sMRI, ML.

1. INTRODUCTION

Autism Spectrum Disorder (ASD) represents an inherited neurodevelopmental condition characterized by various cognitive, social, and communication challenges, often accompanied by related disorders [1]. Typically, ASD manifests in infancy or within the initial three years of childhood [2]. Researchers have explored multiple imaging modalities, such as functional Magnetic Resonance Imaging (fMRI) [3, 4, 5], structural MRI (sMRI) [6, 7], and Diffusion Tensor Imaging (DTI) [8, 9]. This paper concentrates specifically on utilizing fMRI to aid in the objective diagnosis of autism due to its close correlation with individual behavior. fMRI serves as a crucial modality because it accurately assesses synchronization between brain regions within and across hemispheres, pivotal features for potentially facilitating early and objective autism diagnosis. The aforementioned attributes of fMRI form the primary motivation for its utilization within this research. Numerous studies have delved into examining functional connectivity through resting-state fMRI combined with machine learning techniques. In this paper, we will reference the most relevant work to our proposed system due to space constraints. For instance, Nielsen et al. [3] used a leave-one-out linear model classifier to evaluate fMRI data from 396 ASD and 426 typical development patients from ABIDE. They were able to distinguish between autism and typical development with 60% accuracy. Unfortunately, their study did not examine autism severity, which led to relatively low accuracy. Dekhil et al. [4] used resting-state fMRI data from 160 normally developing children and 123 ASD youngsters from NDAR to construct a CAD system for autism diagnosis. Their method used machine learning approaches to attain sensitivity, specificity, and accuracy of about 90%. In a related study [10], employed deep learning on fMRI data from 78 with ASD and 78 with typical development in NDAR, the research was able to obtain an impressive 93% diagnosis accuracy. However, a small sample size and the lack of an assessment of autism severity limit its value. Yang et al. [5] Yang et al. [5] used ABIDE II resting-state fMRI characteristics to differentiate ASD from normally developing people using various machine learning algorithms. They achieved the highest accuracy of 71.98% by combining the Ridge classifier with grid search cross-validation and the CC400 atlas. They, like Nielsen et al., had constraints due to the lack of an assessment of autism severity, resulting in limited accuracy results. Elnakieb et al. [11] presented a method that uses data from 408 ASD and 476 typically developing patients from ABIDEII to diagnose ASD using a combination of resting state-fMRI connectivity analysis and machine learning. One drawback, though, is that precise neurocircuit identification in ASD is hampered by the inability to identify anomalies in recognized brain regions.

Given the aforementioned constraints in analyzing resting-state fMRI in published works, we have developed a diagnostic system with several key capabilities. Firstly, it can distinguish between normally developed brains and those affected by ASD. Secondly, it can determine the severity level of autism in a subject, aiding in classifying their position within the ASD spectrum. Finally, it can identify specific brain regions that demonstrate correlations with ASD, serving as an initial investigation into the abnormal neurocircuits associated with the condition.

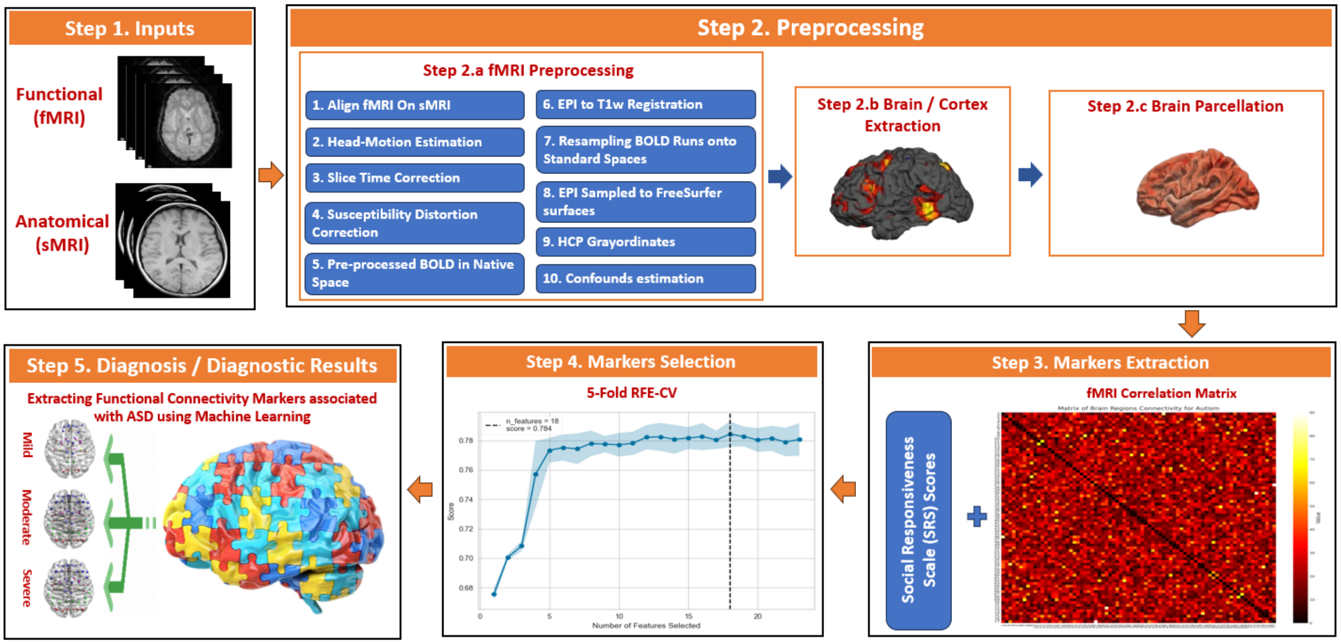

Fig. 1. General AI-based pipeline for processing brain imaging Data for ASD diagnosis

2. MATERIALS & METHODS

The proposed framwork, shown in Fig 1, consists of four main steps: (1) Preprocessing (2) Extracting the functional markers and combining them with SRS scores, (3) Selection of the most significant features relevent to autism, (4) Diagnosis of autism using machine learning.

Material and Subjects: This study involved a cohort of 344 individuals diagnosed with ASD and 374 Typically developing (TD) participants from a total of 13 neurological institutes obtained from a ABIDE II dataset [12] screened utilizing a 3T MRI scanner. For autistic subjects, there are 288 males, and 56 females with mean age of 13.67 and standard deviation of 9.30, for TD subjects, there are 267 males , and 267 females with mean age of 13.71 and standard deviation of 8.73.

Preprocessing: The fMRI preprocessing involved the utilization of FastSurfer [13] and fMRIPrep [14]. This process included various steps: aligning fMRI with sMRI to enhance the localization of functional activations by augmenting fMRI resolution, employing head-motion estimation to strengthen data quality by detecting and rectifying movement-related artifacts and distortions that might compromise subsequent analyses, conducting slice time correction to align slices from different time points and mitigate temporal discrepancies, implementing susceptibility distortion correction to rectify fMRI distortions stemming from magnetic susceptibility variations, and ultimately performing preprocessing of BOLD signals in native space to enhance the BOLD signal data within its original acquisition space.

Brain Extraction: The next step involves the precise extraction of the brain and cortex from the aligned fMRI data. This is accomplished by leveraging spatial information derived from the structural MRI (sMRI), utilizing a probabilistic brain atlas, and considering the visual characteristics of brain tissues. The information obtained from these sources is then input into a Bayesian classifier, which aids in distinguishing between brain tissues and the skull, as shown in Fig 2.

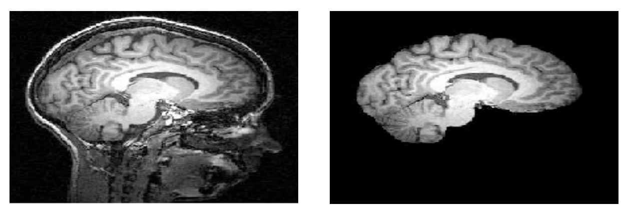

(a) (b)

Fig. 2. Illustration depicting the brain extraction step from fMRI: (a) original images and (b) Extracted brain.

Brain Parcellation: To segment the extracted brain into anatomically similar regions and establish correlations with ASD, enabling the discrimination between ASD and typically developed brains, we employed the MNI152 standard space [15]. This space subdivides the brain cortex into 76 regions per hemisphere, resulting in a total of 152 regions for the entire cortex. To execute this process, we utilized 3D-based affine registration, aligning the extracted brain with the MNI152 standard space, as depicted in Fig 3.

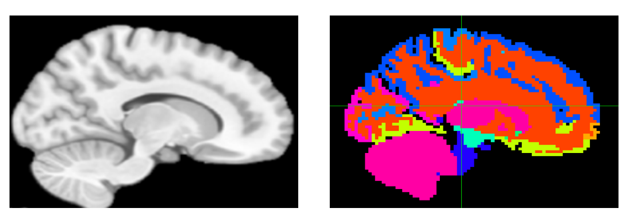

(a) (b)

Fig. 3. Illustration depicting the brain parcellation step from fMRI: (a) standard space and (b) Parcellation.

Connectivity Markers Extraction: The literature [16] reports disruptions in synchronization among different brain regions in individuals with ASD. To precisely identify this abnormal synchronization across brain regions, we devised a novel method to calculate synchronization among all interconnected regions within the same hemisphere, as well as between the hemispheres. This approach aims to detect any potential correlations with ASD across a wide range of brain regions. Utilizing normalized cross as an image radiomic, we represented the synchronization between each pair of interconnected brain regions, shown in Figure 4(a).

Connectivity Markers Selection To pinpoint the brain regions associated with ASD, we employed Recursive Feature Elimination (RFE) in tandem with 5 k-fold cross-validation. This method ensured a thorough and robust selection of markers, maximizing the predictive and diagnostic accuracy of our proposed system. Figure 4(b) illustrates the identified brain regions that exhibit correlation with ASD.

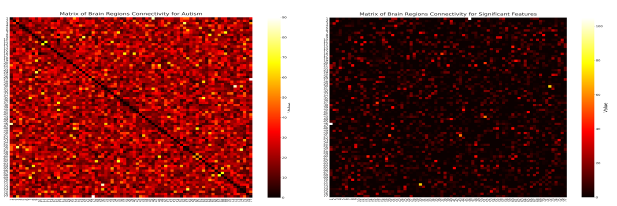

(a) (b)

Fig. 4. Illustration of detected brain regions associated with ASD: (a) The estimated synchronization among all potential mutual brain regions, and (b) the identified brain regions linked to ASD.

3. DIAGNOSIS & MACHINE LEARNING

To identify the most effective classifier that attains the highest accuracy, we conducted experiments using various machine learning models such as logistic regression (LR), linear support vector machine (LSVM), k-nearest neighbors (KNN), gradient boosting (GB), and LightGBM (LGBM). Our aim was to ascertain the classifier that could accurately predict the severity levels of Autism Spectrum Disorder (ASD) including mild, moderate, or severe, as well as distinguish Normal developed brains. The ground truth for these classifications was determined using The Social Responsiveness Scale (SRS) assessment administered by autism experts. As detailed in the experimental section, LSVM emerged as the classifier achieving the highest accuracy. To refine the LSVM model, we utilized Bayesian optimization for fine-tuning its hyperparameters. The hyperparameters of LSVM encompass crucial elements such as regularization parameters, kernel types, and kernel-specific settings, all of which exert a substantial influence on its predictive accuracy. Bayesian optimization simplifies this optimization procedure by employing probabilistic models and iterative decision-making, thereby facilitating a more effective quest for optimal hyperparameters. Through iterative evaluation of LSVM's performance using various hyperparameter combinations, Bayesian optimization strives to enhance the model's predictive capabilities while minimizing the computational resources necessary for hyperparameter tuning.

4. EXPERIMENTAL RESULTS

In this section, we assess the performance of the proposed system on ABIDE II datasets. To ensure robustness and reproducibility, we conducted 40 trials on five folds, as depicted in Table 1. This table illustrates the mean accuracy and standard deviation resulting from these experiments for each severity level, along with the count of connectivity features utilized in each level's experiments. Additionally, Table 2 presents the mean and standard deviation of Sensitivity, Specificity, and Accuracy for each classifier used across feature selection attempts in our experiments. LSVM emerged as the top performer, demonstrating superior results when employed for both feature selection and classification, showcasing its efficacy. Furthermore, logistic regression exhibited commendable performance when utilized simultaneously for feature selection and as a classifier.

Table 1. Mean ± Std. of across all experiments for each severity level with the best classifier's highest accuracy.

Severity Level	# Features	Accuracy
Mild, TD	1414	0.78 ± 0.21
Moderate, TD	1176	0.80 ± 0.18
Severe, TD	1411	0.78 ± 0.17

Table 2. Mean ± Std. of Sensitivity, Specificity, and Accuracy across all experiments for feature selection and each classifier using its optimal hyperparameters.

RFE	ML	Acc	Sens	Spec
lgbm	**gboost**	0.68 ± 0.22	0.41 ± 0.23	0.74 ± 0.29
	knn	0.83 ± 0.06	0.25 ± 0.19	0.94 ± 0.05
	lr	0.84 ± 0.06	0.38 ± 0.24	0.93 ± 0.05
	lsvm	0.84 ± 0.06	0.34 ± 0.25	0.94 ± 0.05
lr	**gboost**	0.64 ± 0.24	0.39 ± 0.29	0.70 ± 0.33
	knn	0.83 ± 0.08	0.35 ± 0.21	0.93 ± 0.10
	lr	0.94 ± 0.05	0.80 ± 0.20	0.98 ± 0.02
	lsvm	0.95 ± 0.04	0.83 ± 0.18	0.98 ± 0.03
lsvm	**gboost**	0.65 ± 0.23	0.37 ± 0.29	0.71 ± 0.33
	knn	0.82 ± 0.09	0.36 ± 0.21	0.92 ± 0.12
	lr	0.95 ± 0.05	0.82 ± 0.20	0.98 ± 0.02
	lsvm	$\mathbf{0.97 \pm 0.04}$	$\mathbf{0.90 \pm 0.16}$	$\mathbf{0.99 \pm 0.02}$

5. CONCLUSION

This study highlights the importance of brain imaging techniques, specifically resting-state fMRI, in the diagnosis of ASD. We suggested a CAD system for autism diagnosis based on functional connectivity obtained from people with autism and typically developing (TD) people from the ABIDEII dataset. By incorporating the Social Responsiveness Scale behavioral report, we were able to categorized autism into 4 levels of (TD, Mild, Moderate, Severe). We executed 40 experiments for each severity level, using Recursive Features Selection and machine learning approaches. Our framework achieved mean accuracy, sensitivity, and specificity of 97%, 90%, and 99%, respectively using 5-fold cross-validation. Future study should investigate the integration of other imaging modalities, such as sMRI and DTI, to provide a deeper understanding of the anatomical abnormalities, functional connectivity, and brain connectivity abnormalities that may have significant effects on autism. Furthermore, combining data from different sources, including genetics, may provide useful insights into the genes that are active in particular people, leading to a better understanding of the core causes driving autism.

6. COMPLIANCE WITH ETHICAL STANDARDS

This study was conducted retrospectively using human subject data made accessible for free by (Autism Brain Imaging Data Exchange II). According to the license attached to the open access data, no ethical approval was required.

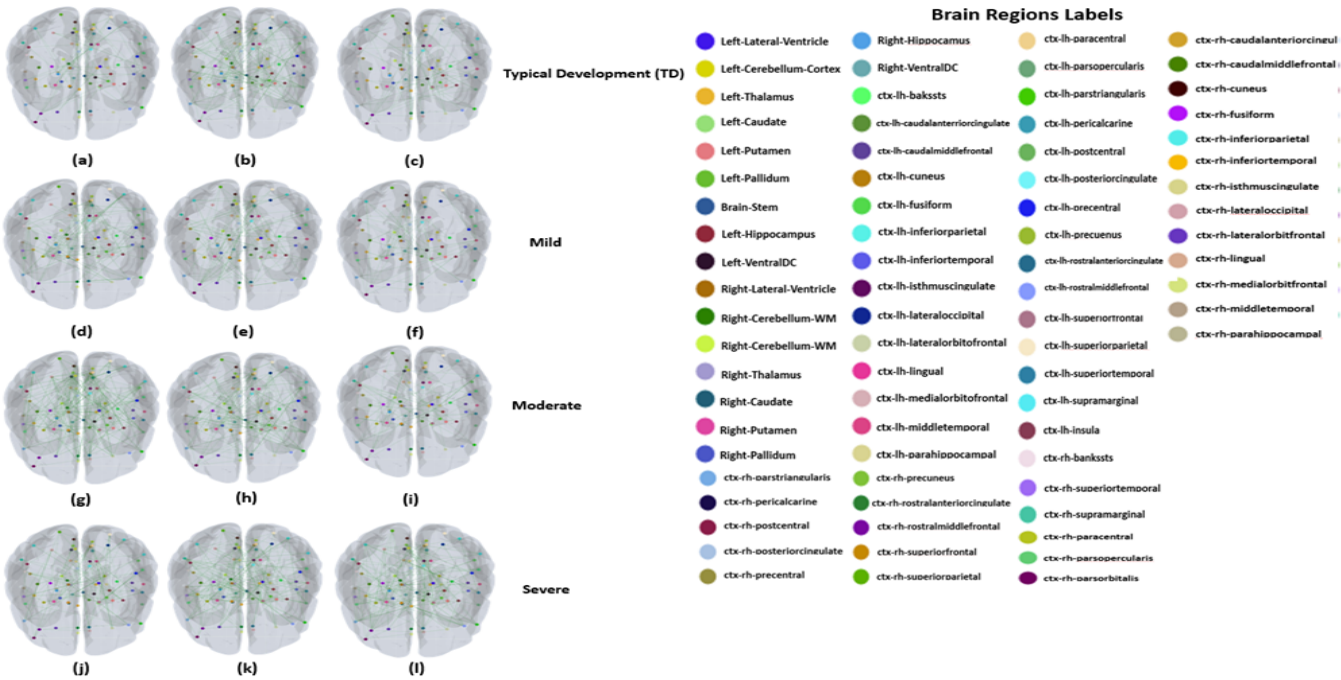

Fig. 5. Connectivity for 3 cases for each level of severity including: typical development, mild, moderate, severe

7. REFERENCES

[1] Svein Eikeseth, "Outcome of comprehensive psycho-educational interventions for young children with autism," *Research in developmental disabilities*, vol. 30, no. 1, pp. 158–178, 2009.

[2] Rebecca J Landa et al., "Developmental trajectories in children with and without autism spectrum disorders: the first 3 years," *Child development*, vol. 84, no. 2, pp. 429–442, 2013.

[3] Jared A Nielsen et al., "Multisite functional connectivity mri classification of autism: Abide results," *Frontiers in human neuroscience*, vol. 7, pp. 599, 2013.

[4] Omar Dekhil et al., "Using resting state functional mri to build a personalized autism diagnosis system," *PloS one*, vol. 13, no. 10, pp. e0206351, 2018.

[5] Xin Yang et al., "Functional connectivity magnetic resonance imaging classification of autism spectrum disorder using the multisite abide dataset," in *2019 IEEE EMBS International Conference on Biomedical & Health Informatics (BHI)*. IEEE, 2019, pp. 1–4.

[6] Mohamed T Ali et al., "Autism classification using smri: A recursive features selection based on sampling from multi-level high dimensional spaces," in *2021 IEEE 18th International Symposium on Biomedical Imaging (ISBI)*. IEEE, 2021, pp. 267–270.

[7] Mohamed T Ali et al., "The role of structure mri in diagnosing autism," *Diagnostics*, vol. 12, no. 1, pp. 165, 2022.

[8] Yaser A Elnakieb et al., "Computer aided autism diagnosis using diffusion tensor imaging," *Ieee Access*, vol. 8, pp. 191298–191308, 2020.

[9] ElNakieb et al., "The role of diffusion tensor mr imaging (dti) of the brain in diagnosing autism spectrum disorder: Promising results," *Sensors*, vol. 21, no. 24, pp. 8171, 2021.

[10] Omar Dekhil et al., "Identifying personalized autism related impairments using resting functional mri and ados reports," in *Medical Image Computing and Computer Assisted Intervention–MICCAI 2018: 21st International Conference, Granada, Spain, September 16-20, 2018, Proceedings, Part III 11*. Springer, 2018, pp. 240–248.

[11] Yaser ElNakieb et al., "Understanding the role of connectivity dynamics of resting-state functional mri in the diagnosis of autism spectrum disorder: A comprehensive study," *Bioengineering*, vol. 10, no. 1, pp. 56, 2023.

[12] Di Martino et al., "Enhancing studies of the connectome in autism using the autism brain imaging data exchange ii," *Scientific data*, vol. 4, no. 1, pp. 1–15, 2017.

[13] Leonie Henschel et al., "Fastsurfer-a fast and accurate deep learning based neuroimaging pipeline," *NeuroImage*, vol. 219, pp. 117012, 2020.

[14] Suzanne Hoogeveen et al., "Religious belief and cognitive conflict sensitivity: A preregistered fmri study," *cortex*, vol. 129, pp. 247–265, 2020.

[15] D Louis Collins et al., "Design and construction of a realistic digital brain phantom," *IEEE transactions on medical imaging*, vol. 17, no. 3, pp. 463–468, 1998.

[16] Christopher S Monk et al., "Abnormalities of intrinsic functional connectivity in autism spectrum disorders," *Neuroimage*, vol. 47, no. 2, pp. 764–772, 2009.